

A Scaling Theory of Clusters in the Lattice Gas

Ronald Dickman¹ and William C. Schieve¹

Received January 25, 1983; revised April 15, 1983 and June 21, 1983

It is proposed that the number of p -particle, k -bond lattice gas cluster configurations is of the form $\exp\{\sigma pf(k/p)\}$ in the limit $p \rightarrow \infty$. A simple modification permits application to finite clusters, with the consequence that asymptotically the cluster partition function is of the droplet form, i.e., $Z_p = \exp[\kappa p - \mu p^{1-1/d} + O(\ln p)]$. The scaling function for two-dimensional lattices is determined numerically and is found to be qualitatively universal. The scaling theory is used to investigate the size dependence of the surface free energy. The surface tension of small clusters can significantly exceed its limiting value. For intermediate cluster sizes (~ 100 particles) there is a modest reduction in surface tension, in accord with Tolman's prediction and the results of recent Monte Carlo studies.

KEY WORDS: Clustering; nucleation; surface tension; statistical geometry.

1. INTRODUCTION

Physical clusters—aggregates of particles bound by an attractive potential—have long been of interest in statistical mechanics. Knowledge of the properties and size distribution of clusters is central to the theory of condensation and metastability, and is essential for predicting the nucleation rate in a supersaturated vapor.^(1,2) Hill⁽³⁾ formulated an expansion of the partition function in terms of physical clusters. Strogyn and Hirschfelder⁽⁴⁾ evaluated the dimer contribution, and Zurek and Schieve⁽⁵⁾ and de la Selva *et al.*⁽⁶⁾ evaluated the trimer, tetramer, and pentamer contributions for the hard core square well model. As with the Ursell–Mayer theory

¹ Center for Studies in Statistical Mechanics, The University of Texas at Austin, Austin, Texas 78712.

which it closely parallels, the rigorous theory of Hill becomes nearly intractable for clusters of more than a few particles, owing to the number and complexity of the integrals encountered. In nucleation theory recourse is often made to a quasithermodynamic approach⁽⁷⁾: the free energy is estimated by treating the cluster as a spherical droplet with bulk and surface free energy densities characteristic of a macroscopic sample of the fluid. Since the critical cluster is generally quite small (10–1000 particles), the accuracy of this “capillarity approximation” is questionable.^(2,8) Indeed, the inadequacy of the capillarity approximation is responsible for the discrepancy (sometimes many orders of magnitude) between observed and predicted nucleation rates.⁽²⁾ Within the context of the droplet picture, the error in the cluster free energy estimate may be interpreted as a symptom of a size-dependent surface tension. This issue has been investigated for several models,^(9–11) but conclusive answers are still lacking.

It would, of course, be most desirable to calculate cluster partition functions *ab initio*, given the intermolecular potential, thereby avoiding macroscopic approximations or assumptions about cluster shapes. Such calculations have been performed for argon clusters at low temperatures.⁽¹²⁾

In view of the difficulties inherent in the microscopic theory of clusters for realistic models, it is natural to turn to the study of clusters in the lattice gas. Aside from relative simplicity, the lattice gas offers many recognized advantages. The bulk phases are well understood on the basis of exact results and/or series expansion, renormalization group, and Monte Carlo studies. Despite obvious oversimplifications, the model appears to capture the essential features of liquid–vapor phase transitions. Comparison between theory and (computer) experiments is detailed and clear-cut: questions which usually complicate the interpretation of nucleation experiments (replacement free energy,^(8,13) ambiguities in bond definition) do not arise. Metastability, clustering, and nucleation in the lattice gas have been studied by Penrose and Lebowitz,⁽¹⁴⁾ who established rigorous bounds on cluster free energies, and by Domb,⁽¹⁵⁾ who examined the analytic properties of a modified droplet model.⁽¹⁶⁾ Among the extensive Monte Carlo simulations of the lattice gas conducted by Binder and his co-workers⁽¹⁷⁾ are a number of studies of cluster properties and of cluster growth dynamics. In a recent study Binder and Kalos⁽¹⁸⁾ examined the size dependence of the surface free energy.

In this paper we calculate cluster partition functions for the lattice gas. Configurations of small clusters may be exhaustively enumerated, permitting an exact evaluation. For larger clusters it is necessary to estimate the number of configurations with a given number of particles and bonds. The importance of this combinatorial problem in the present context seems first to have been recognized by Domb.⁽¹⁵⁾ Our main result is a scaling law

governing the number of cluster configurations. The scaling function appears to be essentially universal for two-dimensional lattices. In addition to shedding light on an intriguing problem of statistical geometry, the theory leads to interesting predictions regarding cluster free energies. In an earlier paper⁽¹⁹⁾ we presented numerical evidence for a scaling law governing the number of cluster configurations in a weak-embedding model. Here we study strong-embedding clusters, i.e., the Ising model. In Section 2 we propose an asymptotic scaling law and consider its extension to finite clusters. Extensive numerical evidence for scaling, largely the result of a new Monte Carlo cluster generation technique, is presented in Section 3. In Section 4 we examine some of the consequences relevant to nucleation theory, and compare our predictions with the results of simulations by Binder and Kalos⁽¹⁸⁾ and Nishioka.⁽⁹⁾

2. SCALING THEORY OF LATTICE GAS CLUSTERS

We consider a cluster—a set of occupied sites connected by nearest-neighbor bonds—in a lattice gas with attractive potential $-\epsilon$. The partition function for a p -particle cluster may be written

$$\tilde{Z}_p = \mathcal{N} \sum_{X | N(X)=p} \xi^{k(X)} \quad (1)$$

where \mathcal{N} is the number of lattice sites,² $\xi = \exp(\epsilon/k_B T)$, and the sum includes exactly one representative from each class of translationally equivalent p -particle cluster configurations. The number of bonds in configuration X is indicated by $k(X)$. Grouping terms according to the number of bonds, we have

$$\tilde{Z}_p = \mathcal{N} Z_p = \mathcal{N} \sum_{k=p-1}^{k_m(p)} \xi^k \sigma_{p,k} \quad (2)$$

The upper limit for the square lattice is

$$k_m(p) = [2(p - \sqrt{p})] \quad (3a)$$

while for the triangle lattice,⁽²⁴⁾

$$k_m(p) = [3p - (12p - 3)^{1/2}] \quad (3b)$$

where $[\]$ indicates the largest integer of its argument. In general,

$$k_m(p) \simeq qp/2 - \chi p^{1-1/d} \quad (4)$$

² We assume that \mathcal{N} is large so boundary effects may be ignored.

for large p in d dimensions, where q is the coordination number and χ a constant which depends on the lattice. In Eq. (2), $\sigma_{p,k}$ is the number of p -particle, k -bond cluster configurations. The quantity $k_B p^{-1} \ln \sigma_{p,k}$ is therefore the entropy density for configurations with internal energy density $-k\epsilon/p$. The main idea of this section is that the entropy density may be expressed as a function of the energy density.

Penrose and Lebowitz⁽¹⁴⁾ established a lower bound on the cluster free energy density, $-k_B T p^{-1} \ln Z_p$. We show in Appendix A that the sequence $(2^n p)^{-1} \ln Z_{2^n p}$ converges to a limit as $n \rightarrow \infty$. In Appendix A we also demonstrate the inequality

$$\sigma_{2p,2k-1} \geq (\sigma_{p,k-1})^2 \quad (5)$$

Let

$$x_n = (np)^{-1} \ln \sigma_{np,nk-1} \quad (6)$$

Iterating Eq. (5), we see that the subsequence x_{2^n} increases monotonically with n . Using the Peierls construction⁽²³⁾ one may place a constant upper bound on $p^{-1} \ln(\sum_k \sigma_{p,k})$, hence on x_m , and so the subsequence x_{2^n} converges. This makes it quite plausible that the sequence x_n has a limit, an assumption we now adopt. By this assumption, the limit, as $p \rightarrow \infty$, and $k \rightarrow \infty$, with the ratio $(k+1)/p$ held constant, of $p^{-1} \ln \sigma_{p,k}$ exists. Then for large p ,

$$\ln \sigma_{p,k} = p \tilde{f} \left(\frac{k+1}{p} \right) + o(p) \quad (7)$$

Using the inequality (proved in Appendix A),

$$\sigma_{2p,k} \geq \sigma_{p,k'} \sigma_{p,k-k'-1} \quad (8)$$

and Eq. (7) in the limit of large p , we find

$$\tilde{f}(z) \geq \frac{1}{2} [\tilde{f}(z+y) + \tilde{f}(z-y)] \quad (9)$$

where $z = (k+1)/2p$ and $y = (k-2k'-1)/2p$. Equation (9) suggests that \tilde{f} is concave (and thereby continuous) on the interval $[1, q/2)$, properties we shall henceforth assume. Under the continuity assumption Eq. (7) simplifies slightly to

$$\ln \sigma_{p,k} = p \tilde{f} \left(\frac{k}{p} \right) + o(p) \quad (10)$$

in the limit $p \rightarrow \infty$. It is convenient to introduce a scaled bond number

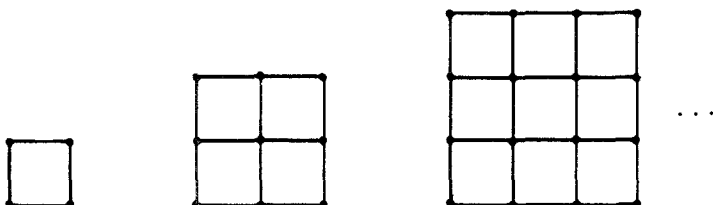
$$\tilde{x} = \frac{(k/p) - 1}{(q/2) - 1} \quad (11)$$

Equation (10) may then be put in the form

$$\ln \sigma_{p,k} = \sigma p f(\tilde{x}) + o(p) \tag{12}$$

where σ is a constant chosen so that f attains a maximum value of 1.

We now consider the extension of the scaling hypothesis to include the cluster surface. We shall attempt to account for surface effects by modifying the scaling variable \tilde{x} . In the square lattice (an analogous construction can be made for any other lattice), the configurations with the maximum number of bonds per particle form the sequence



with $p = p^*(n) = n^2$ and $k = k^*(n) = 2n(n - 1)$ ($n = 1, 2, 3, \dots$). For each n there is a unique p^* -particle, k^* -bond cluster configuration, and so $\sigma_{p^*,k^*} = 1$ for each n . If we write

$$\sigma_{p,k} = \exp\{\sigma p f[x(p,k)]\} \tag{13}$$

then we must have $x(p^*,k^*) = x^*$, where $f(x^*) = 0$. (We assume that the scaling function has a single zero in the region of interest.) The simplest generalization of Eq. (11) which always takes the same value when $p = p^*(n)$ and $k = k^*(n)$ is

$$x(p,k) = \frac{k - p + 1}{p - 2\sqrt{p} + 1} \tag{14a}$$

Then $x \in [0, 1]$, $x(p, p - 1) = 0$, and $x^* = 1$. Note that as $p \rightarrow \infty$ and $k \rightarrow \infty$ with k/p fixed, $x(p,k) \rightarrow \tilde{x}(p,k)$. The condition $x(p^*,k^*) = x^*$ is also satisfied by

$$\frac{k - p + 1}{p - 2p^{\zeta(p,k)} + 1}$$

so long as $\zeta(p,k) \rightarrow 1/2$ when $k \rightarrow k_m(p)$. We will see that the surface free energy of a p -mer grows as p^ζ . While the cluster surface area grows as $p^{1-1/d}$ at low temperature, there is probably a crossover⁽¹⁵⁾ at a higher

temperature to a regime where ramified clusters (whose surface area grows $\sim p$), dominate. However, the cross-over temperature is unknown, and the use of a variable surface exponent introduces a new level of complexity into the numerical analysis of scaling. We assume the surface energy of a p -mer grows as $p^{1-1/d}$ and adopt Eqs. (13) and (14a) as a working hypothesis, bearing in mind that some of our conclusions may be valid only at low temperatures.

An argument similar to the one leading to Eq. (14a) gives

$$x(p, k) = \frac{k - p + 1}{2p - (12p - 3)^{1/2} + 1} \quad (14b)$$

for the triangle lattice, and to the general form

$$x(p, k) \simeq \frac{k - p + 1}{q'p - \chi p^{1-1/d} + 1} \quad (15)$$

for large p , where $q' = q/2 - 1$. Equation (13) may be further generalized by replacing σp with

$$\sigma_0(p) = \sigma p - \theta \ln p + c \quad (16)$$

This modification is necessitated by the asymptotic behavior

$$\sigma_T(p) \equiv \sum_k \sigma_{p,k} \simeq p^{-\lambda} \exp(\sigma p + b) \quad (17)$$

with $\lambda \simeq 1$ in two dimensions, as shown by Sykes and Glen.⁽²⁰⁾ In principle we could write Eq. (16) with $\theta = \theta(x)$, but our present knowledge is not sufficient to determine whether θ has any x dependence. It will turn out that the scaling form

$$\sigma_{p,k} \simeq \exp[\sigma_0(p)f(x)] \quad (18)$$

can fit the data very well, so that corrections due to x dependence of θ are small.

The scaling assumption yields a cluster free energy with bulk and surface terms, regardless of the precise form of $f(x)$. Approximating Eq. (2) by an integral in the limit of large p , and using Eqs. (15), (16), and (18), we may write the partition function as

$$\begin{aligned} Z_p = & (q' - \chi p^{-1/d}) p \\ & \times \int_0^1 dx \exp \left(p \left\{ \left(\sigma - \frac{\theta \ln p - c}{p} \right) f(x) \right. \right. \\ & \left. \left. + [(q' - \chi p^{-1/d} + p^{-1})x + 1 - p^{-1}] / T^* \right\} \right) \quad (19) \end{aligned}$$

where $T^* = k_B T / \epsilon$. Assume that f is differentiable and that $g = (f')^{-1}$ (the inverse of df/dx) exists and is differentiable. Let \tilde{x} be the point where the integrand takes its maximum, i.e.,

$$\left. \frac{df}{dx} \right|_{x=\tilde{x}} = - \frac{q' - \chi p^{-1/d} + p^{-1}}{[\sigma - (\theta \ln p - c)/p] T^*} \tag{20}$$

or,

$$\tilde{x}(T^*, p) = g \left\{ - \frac{q' - \chi p^{-1/d} + p^{-1}}{[\sigma - (\theta \ln p - c)/p] T^*} \right\} \tag{21}$$

Expanding Eq. (19) about this point, we find, for large p ,

$$\ln Z_p = \kappa p - \mu p^{1-1/d} + \nu p^{1-2/d} + \left(\frac{1}{2} - \theta f(\tilde{x})\right) \ln p + D + O p^{-1/d} \tag{22}$$

where

$$\kappa = \sigma f(\tilde{x}) + (q' \tilde{x} + 1) / T^* \tag{23}$$

$$\mu = \chi \tilde{x} / T^* \tag{24}$$

$$\nu = - \frac{\chi^2}{2\sigma T^{*2} f''(\tilde{x})} \tag{25}$$

and

$$D = c f(\tilde{x}) - (1 - \tilde{x}) / T^* + \frac{1}{2} \ln \{ 2\pi q'^2 / \sigma [- f''(\tilde{x})] \} \tag{26}$$

and where $\tilde{x}(T^*) = \lim_{p \rightarrow \infty} \tilde{x}(T^*, p)$. Thus the cluster free energy, $-k_B T \ln Z_p$, has the expected form for large p , and $-k_B T \kappa$ is the bulk free energy per particle. We define the surface free energy of a p -mer as

$$F_p^s = -k_B T (\ln Z_p - \kappa p) \simeq k_B T \mu p^{1-1/d} \quad (p \rightarrow \infty) \tag{27}$$

At low temperatures the surface area A_p of a p -mer is proportional to $p^{1-1/d}$, and may be written

$$A_p = \mathcal{A} (p/\rho)^{1-1/d} \tag{28}$$

where ρ is the bulk number density in the cluster and \mathcal{A} is a geometrical factor which depends on the equilibrium shape of a large cluster. The surface tension is

$$\gamma_s = \lim_{p \rightarrow \infty} F_p^s / A_p = (k_B T / \mathcal{A}) \mu \rho^{1-1/d} \tag{29}$$

The internal energy per particle is given by

$$u = \lim_{p \rightarrow \infty} \frac{(k_B T)^2}{\epsilon} \frac{\partial}{\partial T^*} p^{-1} \ln Z_p = -\epsilon (q' \tilde{x} + 1) \tag{30}$$

and the specific heat per particle is

$$c = \frac{du}{dT} = -q' k_B \frac{d\bar{x}}{dT^*} = -\frac{k_B q'^2}{\sigma T^{*2}} \left(\frac{d^2 f}{dx^2} \Big|_{x=\bar{x}} \right)^{-1} \quad (31)$$

since $g = (f')^{-1}$. The assumed concavity of f implies $c \geq 0$. Furthermore,

$$\frac{d^2 f}{dx^2} \Big|_y < 0 \quad (32)$$

if, at the temperature T^* for which $\bar{x}(T^*) = y$, the specific heat is finite. If $f'' = 0$ in the interval (x_1, x_2) (and is negative outside this interval), then there is a temperature T' such that $\bar{x}(T'^+) = x_1$, and $\bar{x}(T'^-) = x_2$, so there is a first-order phase transition at T' . If f'' vanishes at an isolated point there is a second-order transition. For $f'(\bar{x}) = -q'/\sigma T^*$ to have a solution for all T^* , $f'(x)$ must diverge as $x \rightarrow 1$. If $f'(1)$ were finite, then for all T^* less than some $T_0^* > 0$, $\bar{x} = 1$, implying that the specific heat vanishes at T_0^* , which is unphysical. We therefore expect that $f'(x) \rightarrow -\infty$ as $x \rightarrow 1$. Similarly, if the specific heat is to be nonzero at all finite (high) temperatures, $f'(x)$ must vanish at some point in $[0, 1)$.

We have seen that the scaling hypothesis—which proposes a simple relationship between the cluster entropy and energy densities—is mathematically well motivated and leads to reasonable physical consequences. In the following section the scaling hypothesis is tested numerically.

3. NUMERICAL EVIDENCE FOR SCALING

We have made a detailed study of $\sigma_{p,k}$ for strong embeddings in two-dimensional lattices, using both exact enumeration and Monte Carlo techniques. As is well known, the exhaustive enumeration approach is limited to fairly small ($p \lesssim 15$) clusters, owing to the rapid proliferation of graph topologies. An important exception is the case of maximally bonded (or nearly maximally bonded) clusters, since their number is relatively small. Such clusters may be enumerated using a duality relation between lattice animals. We have generated “by hand” nearly complete tables of $\sigma_{p,k}$ for $p \leq 9$ for the triangle lattice and for $p \leq 11$ for square lattice embeddings.

A Monte Carlo program is used to determine $\sigma_{p,k}$ for $p \gtrsim 30$. Our Monte Carlo cluster generation technique is a modification of a method proposed by Ziff.⁽²¹⁾ With the origin initially occupied, a cluster is grown by “testing” the sites adjacent to it: each is occupied independently with probability z . Once all the neighbors of the origin have been tested, one of the newly occupied sites is chosen at random to serve as the next “testing site”—its nearest neighbors (those as yet untested) are tested in sequence.

Once all of the nearest neighbors of this site have been tested, a new testing site is selected from the set of occupied sites which have not yet served as testing site. The growth process ends as soon as p sites are occupied, or when no new testing site is available. (In this case the result is discarded and a new attempt to grow a p -mer is initiated.) The value of this technique is that it always generates a connected cluster with a specified number of points.

It is shown in Appendix B that the quantity

$$S_{p,k} = \sum_{(p,k)} w(r) \tag{33}$$

(sum over all realizations of p -point, k -line clusters) converges to $A\sigma_{p,k}$, with A independent of k . In Eq. (33) the weight factor is

$$w(r) = (1 - z)^{-u} \tag{34}$$

where u is the number of sites tested and found unoccupied.

The chief limitation of this Monte Carlo technique is its inability to generate compact (i.e., nearly maximally bonded) clusters when $p \gtrsim 25$. By forcing the growth process to spiral outward from the origin, and by making $z \simeq 1$, it is possible to generate many compact clusters. But then the denominator in Eq. (34) becomes very small, and large fluctuations render the results worthless. Clusters with $k_m(p)$, $k_m(p) - 1$, and in some cases $k_m(p) - 2$ bonds are enumerated by hand, but for $p \gtrsim 30$ there is a significant gap in the results. In our calculations we used $z = 0.45$ for the triangle and square lattices, and $z = 0.7$ for the hexagon lattice. For each value of p we performed five runs, each involving 10^6 cluster realizations.

A is eliminated from our results by noting that

$$\sum_k S_{p,k} = A\sigma_T(p)$$

and using accurate estimates of $\sigma_T(p)$ [Eq. (15)] obtained from the data of Sykes and Glen,⁽²⁰⁾ as described in Appendix C.

To analyze the scaling behavior of $\sigma_{p,k}$ we define

$$f_p(x) = \ln \sigma_{p,k} / \tilde{\sigma}_0(p) \tag{35}$$

where

$$\tilde{\sigma}_0(p) = \ln \sigma_{p,\bar{k}} / f[x(p, \bar{k})] \tag{36}$$

(\bar{k} is the value of k which maximizes $\sigma_{p,k}$). If we replace $f(x)$ with $f_p(x)$ and use Eq. (36) for $\sigma_0(p)$ then Eq. (16) is exact. Of course Eq. (36) requires that we know $f(x)$. But since $f[x(p, k)] \cong 1$ (f' vanishes near this point), we can use $\sigma_0(p) = \ln \sigma_{p,\bar{k}}$ as a very good first approximation.

Based on the arguments of Section 2, we expect that $f(x) \in [0, 1]$, that $f(1) = 0$, $f'(1) = -\infty$, $f'(x_0) = 0$ for some $x_0 \in [0, 1)$, and that f is concave

Table I.

	p	γ	η	x_0
Square lattice	15	0.68	± 0.04	1.51
	20	0.65	0.04	1.38
	25	0.66	0.03	1.42
	30	0.67	0.03	1.43
	32	0.665	0.04	1.42
Triangle lattice	10	0.56	± 0.08	1.31
	15	0.59	0.04	1.37
	19	0.59	0.05	1.34
	22	0.58	0.06	1.29
	25	0.61	0.06	1.35
Hexagon lattice	24	0.7	± 0.02	1.40
	32	0.72	0.04	1.45

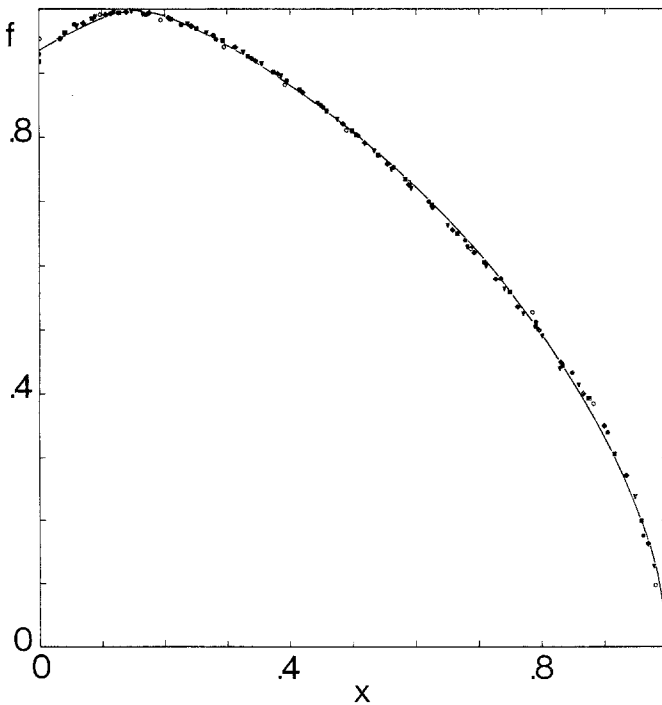


Fig. 1. $f_p(x)$ vs. x for the triangle lattice. Open circles, $p = 10$; solid circles, $p = 15$; squares, $p = 19$; diamonds, $p = 22$; triangles, $p = 25$. The solid line is Eq. (37) with the $p = 19$ best-fit parameters. (Error bars are smaller than or equal to the size of the symbols.)

and differentiable for $x \in [x_0, 1)$. A simple function with these properties is

$$f(x) = \left[1 - \left(\frac{|x - x_0|}{1 - x_0} \right)^\eta \right]^\gamma \tag{37}$$

with $\eta > 1$ and $0 < \gamma < 1$. Preliminary analysis of $f_p(x)$ for $p \leq 12$ indicates that the data may be fit fairly well with $\eta \simeq 1.5$ and $\gamma \simeq 2/3$.

To get precise estimates for x_0 , γ , and η , we find the set of parameters which, for a given p , minimizes the sum of the squares of the distances between the points $f_p(x)$ and the curve $f(x)$. Included in the analysis are all points with $k > \bar{k}$. (The regime $k < \bar{k}$ is of little physical interest.) The best-fit parameters³ are given in Table I.

The known values of $f_p(x)$ for the triangle lattice are plotted in Fig. 1. The solid line is given by Eq. (37) with the $p = 19$ best-fit parameters. Figure 2 is a similar plot for the square lattice using the $p = 25$ parameters.

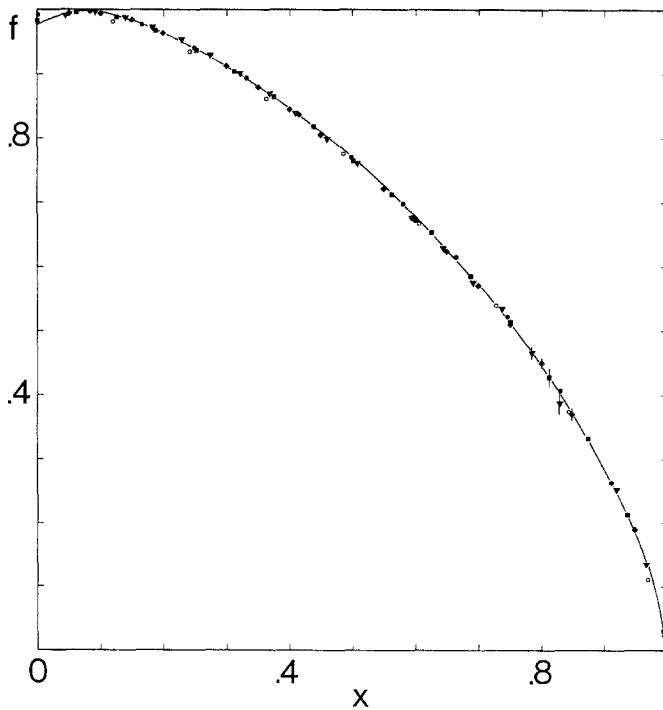


Fig. 2. $f_p(x)$ vs. x for the square lattice. Open circles, $p = 15$; solid circles, $p = 20$; squares, $p = 25$; diamonds, $p = 30$; triangles, $p = 32$. The solid line is Eq. (37) with the $p = 25$ best-fit parameters.

³ The uncertainties in the best-fit parameters reflect variations over which the root-mean-square distance from f to the data points is less than or equal to twice its minimum value.

From Table I and the figures it is evident that (i) finite p scaling holds to very good approximation for p in the range of 20–32 in the square lattice, and for $p = 15$ –25 in the triangle lattice; (ii) the scaling function $f(x)$, Eq. (37), fits the available data very well⁴; (iii) the exponents γ and η are rather insensitive to lattice structure. To within the uncertainties of the estimates, η is in fact lattice invariant.

The form of the scaling function and the approximate “universality” of the scaling parameters reflect, we believe, some more fundamental combinatorial-geometrical principle. While data for larger clusters will be required to determine $f(x)$ to high precision, our results leave little doubt of the validity of the scaling theory.

4. CLUSTER PROPERTIES

In this section we consider some applications of the scaling theory of clusters. A prime motivation for the study of clusters derives from the theory of homogeneous nucleation of a liquid–vapor phase transition.^(1,2) In the classical theory it is assumed that the free energy of formation of a cluster of p particles is given by

$$\Delta W_p^f = p\Delta g + \gamma_s s(p/\rho)^{1-1/d} \quad (38)$$

where Δg is the difference in the bulk phase free energies (per particle) and γ_s is the surface tension. As has often been noted,^(2,5,6) this “capillarity approximation” is of doubtful validity for small clusters. Since even a 10% change in surface tension can alter the nucleation rate by orders of magnitude, the size dependence of the surface tension is of great interest.

Consider the surface free energy per particle

$$\mu_p = \frac{F_p^s}{k_B T p^{1-1/d}} \quad (39)$$

From Eqs. (22) and (26) we see that

$$\mu_p = \mu - \left[\frac{1}{2} - \theta f(\bar{x}) \right] \ln p/p^{1-1/d} - \nu/p^{1/d} - D/p^{1-1/d} + O(1/p) \quad (40)$$

for large p . To evaluate the parameters θ and c we note that

$$\begin{aligned} \sigma_T(p) &\simeq e^{\sigma p + b}/p^\lambda \simeq q' p \int_0^1 dx \exp[(\sigma p - \theta \ln p + c)f(x)] \\ &\simeq 2q' p \Gamma(1/\eta) \eta^{-1} (\gamma a \sigma p)^{-1/\eta} \exp(\sigma p - \theta \ln p + c) \end{aligned} \quad (41)$$

⁴ The error in the fit is typically about 0.5%. This error is not simply a result of numerical uncertainties, for $\ln \sigma_{p,k}$ is typically known to within about 0.1% (except in the range $x = 0.7$ – 0.9 where the Monte Carlo statistics are poor).

for large p , if $f(x)$ is given by Eq. (37), and where $a = (1 - x_0)^{-\eta}$. Thus

$$\theta = \lambda + 1 - \eta^{-1} \tag{42}$$

and

$$c = b + \eta^{-1} \ln(\gamma a \sigma) - \ln[2\Gamma(1/\eta)/\eta] \tag{43}$$

In two dimensions the leading correction to μ_p for large p is due to the term $\sim \ln p/\sqrt{p}$. Since $\lambda \simeq 1$, and $\eta \simeq 1.4$, $\theta \simeq 1.29$. The coefficient of $\ln p/\sqrt{p}$ in Eq. (40) is positive for $T^* < 0.47$. $f(\bar{x})$ decreases with T^* , so this correction is most significant at fairly low temperatures. (However, when $T \rightarrow 0$, $F_p^s/\sqrt{p} \geq 2$.)

In the square lattice, the reduction in μ_p at $T^* = 0.25$ is greatest for $p = 120$, where it amounts to about 1%; for $T^* = 0.5$ the maximum reduction is only about 0.1%. (The critical temperature of the square lattice gas is $T_c^* \simeq 0.5673$.) The scaling theory predicts that for small p , μ_p is somewhat greater than its asymptotic value. $T^*\mu_p$ for square lattice clusters is plotted as a function of p for three temperatures in Fig. 3. The scaling theory parameters $\gamma = 0.655$, $\eta = 1.4$, and $x_0 = 0.085$ have been used.

The size dependence of the surface tension is qualitatively similar for other two-dimensional lattices, and is not very sensitive to the details of the scaling function. In Ref. 20 we arrived at similar conclusions regarding the behavior of μ_p for a weak-embedding model with a rather different form for $f(x)$.

The same qualitative behavior in μ_p was found by Nishioka⁽⁹⁾ to

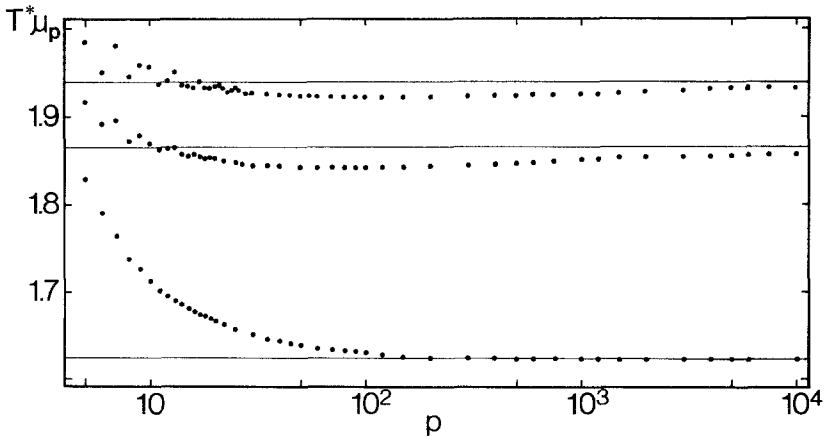


Fig. 3. Surface free energy density, $T^*\mu_p$, calculated from the scaling theory, versus p , for three temperatures. Upper set, $T^* = 1/4$; middle set, $T^* = 1/3$; lower set, $T^* = 1/2$. $\mu(T^*)$ is indicated by a horizontal line.

obtain in computer simulations of (three-dimensional) argon clusters: for small clusters there is a significant enhancement, and for large clusters a modest reduction in the surface tension. Again the small- p enhancement is more significant at high temperatures and the large- p reduction is more pronounced at lower T .

Nishioka found that the data for μ_p could be fit by functions of the form

$$\mu_p = \mu - a/p^{1/3} + b/p^{2/3} \quad (44)$$

From Eq. (40) we see that in three dimensions, $\mu_p = \mu - \nu/p^{1/3} + O(\ln p/p^{2/3})$ so that the leading correction predicted by scaling theory agrees with the Tolman-like correction found by Nishioka. Note that all thermodynamically admissible scaling functions (i.e., $f'' < 0$) lead to $\nu \geq 0$, by Eq. (25). The parameter ν , which is proportional to the specific heat, vanishes when $T \rightarrow 0$. As in the two-dimensional case we expect no Tolman correction for microcrystals. This is consistent with the results of Lee *et al.*,⁽¹⁰⁾ who found no such correction for microclusters at low T .

Tolman⁽²²⁾ gave a thermodynamic argument suggesting that the surface tension of a droplet of radius r would be smaller than its asymptotic value by a factor

$$\gamma_s(r)/\gamma_s(\infty) = 1/(1 + 2\delta/r) \quad (45)$$

where δ is the difference in the radii of two dividing surfaces—the Gibbs surface of tension and the surface of “vanishing superficial density.” If δ is independent of cluster size, the resulting correction is in accord with that found by Nishioka, and predicted by our theory. But if we carry over this assumption to two dimensions, we find

$$\mu_p/\mu \simeq 1 - O(1/\sqrt{p}) \quad (46)$$

which disagrees with the scaling theory prediction, Eq. (40). The enhancement of μ_p for small clusters is not predicted by Tolman’s analysis, since it reflects fluctuations of the cluster from its equilibrium shape.

In addition to studying the properties of isolated clusters, we may apply the scaling theory to the calculation of the cluster size distribution in a liquid–vapor system. We consider here the square lattice gas studied in the Monte Carlo simulations of Binder and Kalos.⁽¹⁸⁾ The system consists of a fixed number of particles, P , on a lattice of N sites. In the simulations, P , N , and T are such that the equilibrium state consists of a single large cluster of p^* particles surrounded by a vapor of monomers and small clusters. If $P/N \ll 1$ we may, to good approximation, neglect excluded volume effects. Then the canonical partition function may be expressed as

a sum of products of cluster partition functions

$$Q(N, P, T) = \sum_{N_1} \sum_{N_2} \cdots \sum_{N_p} \prod_n \frac{(NZ_n)^{N_n}}{N_n!} \tag{47}$$

N_p is the number of p -mers in the system, and the sum is restricted by the condition $\sum_p pN_p = P$. In evaluating Q we use exact series expansions to evaluate the partition functions of small clusters, and scaling theory for $p \geq 20$. For $P = 120$, $N = 3600$, and $T^* = 1/3$, Binder and Kalos found $\langle p^* \rangle \cong 102$ and $\langle N_1 \rangle \cong 12$, while the scaling theory predicts $\langle p^* \rangle = 105.6$ and $\langle N_1 \rangle = 10.6$. The scaling theory predictions are rather insensitive to small changes in the scaling parameters.

Binder and Kalos were also able to estimate the derivative of the surface free energy with respect to cluster size. Using the scaling theory, we compute

$$\left. \frac{\partial F_p^s}{\partial p} \right|_T \simeq \frac{1}{2} (F_{p+1}^s - F_{p-1}^s)$$

Theory and experiment are compared in Fig. 4. The scaling theory is seen to be in excellent agreement with the data, while the capillarity approxima-

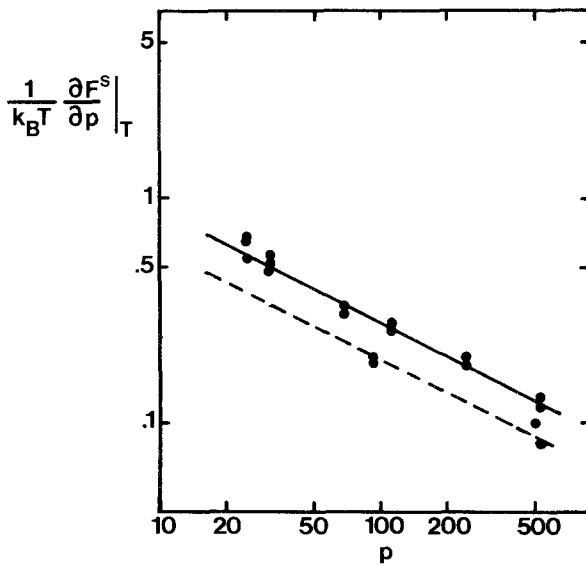


Fig. 4. $(k_B T)^{-1}(\partial F_p^s / \partial p)_T$ vs. p . Dots are from simulation of Binder and Kalos, Ref. 18. The solid line is the scaling theory prediction, and the dashed line is obtained using the capillarity approximation.

tion is clearly wrong. [It must be noted, however, that the capillarity approximation fails in part because the surface tension of a plane (10) interface is employed in the calculation; the surface tension is greater for other orientations.]

ACKNOWLEDGMENTS

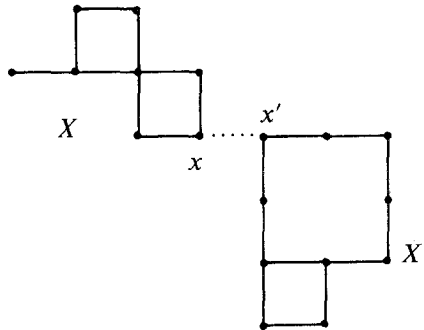
We are grateful to Bill Wooters, Wojciech Zurek, Charles Radin, Jack Swift, Dietrich Stauffer, and Charles Newman for helpful and informative discussions. R.D. wishes to thank the Robert A. Welch Foundation for partial support.

APPENDIX A: INEQUALITIES FOR Z_p AND $\sigma_{p,k}$

From Eqs. (1) and (2) we have that

$$Z_p Z_{p'} = \sum_{\substack{X, X' \\ N(X)=p, N(X')=p'}} \xi^{k(X)+k(X')} \tag{A1}$$

Now for each pair $\{X, X'\}$ in the sum we can construct a cluster configuration X'' with $p + p'$ points and $k(X) + k(X') + 1$ lines as follows. Let x be the point in X furthest to the right and lowest in X , and let x' be the point furthest to the left and highest in X' . To form X'' , place x immediately to the left of x' , and join these points by a line:



For each pair $\{X, X'\}$ we obtain a distinct X'' . Thus there is a 1 : 1 correspondence between terms in the sum Eq. (A2) and a subset of the terms in $Z_{p+p'}$. (For $p + p' \geq 4$ there are configurations in $Z_{p+p'}$ which cannot be constructed from $\{X, X'\}$ pairs.) Moreover, the term X'' in $Z_{p+p'}$

corresponding to $\{X, X'\}$ in $Z_p Z_{p'}$ is multiplied by an additional factor of $\xi \geq 1$. Hence

$$Z_{p+p'} \geq Z_p Z_{p'} \tag{A2}$$

so that

$$(2p)^{-1} \ln Z_{2p} \geq p^{-1} \ln Z_p \tag{A3}$$

Using a Peierls argument⁽²³⁾ one may place a constant upper bound on $p^{-1} \ln Z_p$. For instance, for the square lattice Penrose and Lebowitz⁽¹⁴⁾ showed that

$$p^{-1} \ln Z_p \leq 2(\ln 3 + \epsilon/k_B T) \tag{A4}$$

Equations (A3) and (A4) imply that $\lim_{n \rightarrow \infty} (2^n p)^{-1} \ln Z_{2^n p}$ exists.

Our construction generates a 1 : 1 correspondence between the set of pairs of cluster configurations (one member having p particles and k bonds, the other p' and k'), and a subset of the configurations with $p + p'$ particles and $k + k' + 1$ bonds. Thus

$$\sigma_{p+p', k+1} \geq \sum_{k'} \sigma_{p, k'} \sigma_{p', k-k'}$$

and so

$$\sigma_{2p, k} \geq \sigma_{p, k'} \sigma_{p, k-k'-1} \tag{A5}$$

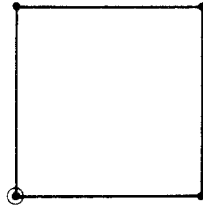
which is Eq. (8), and, with a simple rearrangement, gives Eq. (5).

APPENDIX B: MONTE CARLO CLUSTER GENERATION

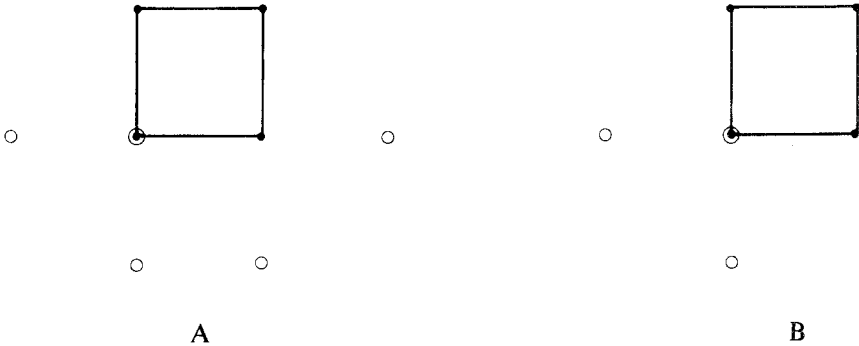
The Monte Carlo scheme generates realizations of cluster configurations. If $\{x\}$ is the set of p points in a cluster configuration C , ($x \in \{x\} \Rightarrow x \in Z^d$, and $0 \in \{x\}$), then a realization of C is an ordering of these points, i.e., the order in which these lattice sites are occupied in the cluster generation process. Thus 0 is always first in the realization, and the second point is one of the nearest neighbors of 0.

The outcome of the cluster generation process is determined by two kinds of random events. One is the occupation, each independently and with probability z , of sites adjacent to a certain occupied site, called the "testing site." (The neighbors of this site are always tested in a fixed order, e.g., counterclockwise, starting with the point directly below the testing site.) The testing site is itself chosen at random from the set of occupied sites which have not yet served as the testing site. Thus there are in general several possible realizations of a given cluster configuration, i.e., several

possible sequences of testing sites which lead to the same configuration. For instance, there are two possible realizations of the configuration



(The circled point is 0.) After testing the neighbors of 0, either (1, 0) (case A), or (0, 1) (case B) may be chosen as the next testing site. Note that the number of unoccupied sites, u , is different in the two realizations. In case B two of the neighbors of the testing site (0, 1) remain untested since the growth process terminates once p (in this case 4) sites have been occupied.



(An open circle denotes a site tested and found unoccupied.) Given that some four-particle cluster is realized, the probability that realization (A) occurs is

$$P(A) = (1/2)(1 - z)^4 / \sum_r P(r)$$

and the probability that (B) occurs is

$$P(B) = (1/2)(1 - z)^2 / \sum_r P(r)$$

The factor of 1/2 represents the fact that (0, 1) and (1, 0) are equally likely to be chosen as the next testing site after 0. The relative probability of an

arbitrary realization r is

$$(1 - z)^{u(r)} \prod_j (1/n_j)$$

where n_j is the number of sites from which the j th testing site is chosen.

Given a cluster configuration we may find all its possible realizations by enumerating the different sequences of testing sites. A testing site sequence assigns labels $1, 2, \dots, q$ ($q \leq p - 1$) to certain points in C , subject to the following rules:

- (1) 0 is labeled "1."
- (2) If point x is labeled j , then one of the sites adjacent to x is labeled $i < j$.
- (3) Every site is either labeled or is adjacent to a labeled site, and this condition is first satisfied when the label " q " is assigned.

Consider a process which randomly generates labelings of a certain C according to these rules. The probability of obtaining a particular realization $r(C)$ is

$$\prod_{j=2}^{q(r)} 1/n_j(r)$$

Hence

$$\sum_{r(C)} \prod_{j=2}^{q(r)} 1/n_j(r) = 1 \tag{B1}$$

The expectation of the sum $\sum_{r(C)} w(r)$ is therefore

$$E \sum_{r(C)} w(r) = Y \sum_{r(C)} P(r) (1 - z)^{-u(r)} = Y \tag{B2}$$

where Y depends on z, p , and the total number of Monte Carlo trials. Each translationally nonequivalent cluster configuration can occur in p equivalent ways (there are p choices for the particle which occupies 0). Thus

$$E \sum_{\substack{\text{(all realizations of} \\ p\text{-particle, } k\text{-bond} \\ \text{configurations)}}} w(r) = Yp \sum_{T(p,k)} \alpha(T)/s(T) = A\sigma_{p,k} \tag{B3}$$

APPENDIX C: ESTIMATION OF $\sigma_T(p)$

Sykes and Glen⁽²⁰⁾ have calculated $\sigma_T(p) = \sum_k \sigma_{p,k}$ for $p \leq 16$ for the triangle lattice, $p \leq 19$ for the square lattice, and $p \leq 22$ for the hexagon lattice. Their Padé approximant analysis indicates that asymptotically

$$\sigma_T(p) \simeq B \frac{e^{\sigma p}}{p^\lambda} \tag{C1}$$

with $\lambda \simeq 1$. This asymptotic behavior implies that the ratios of successive $\sigma_T(p)$ values are well-approximated by

$$\omega_p = \frac{\sigma_T(p)}{\sigma_T(p-1)} \simeq e^{\sigma} \left(1 - \frac{\lambda}{p}\right) \quad (\text{C2})$$

To extrapolate $\sigma_T(p)$ for the triangle and hexagon lattices we use Eq. (C2) with $\lambda = 1$. This formula is accurate to within 0.1% for the last three exactly known ratios. For the square lattice we find a better fit ($< 0.03\%$ error for last four ratios) if we modify Eq. (C2) to

$$\omega_p \simeq e^{\sigma} \left[1 - 1/(p + 0.85)\right] \quad (\text{C3})$$

Eqs. (C2) and (C3) are used in conjunction with the following results from Ref. (20):

$$\left. \begin{array}{l} \sigma = 1.646 \pm 0.006 \\ \sigma_T(16) = 4\,474\,080\,844 \end{array} \right\} \text{triangle lattice}$$

$$\left. \begin{array}{l} \sigma = 1.401 \pm 0.005 \\ \sigma_T(19) = 5\,940\,738\,676 \end{array} \right\} \text{square lattice}$$

$$\left. \begin{array}{l} \sigma = 1.112 \pm 0.007 \\ \sigma_T(22) = 728\,445\,773.5 \end{array} \right\} \text{hexagon lattice}$$

REFERENCES

1. R. Becker and W. Döring, *Ann. Phys. (Leipzig)* **24**:719 (1935); J. Frenkel, *J. Chem. Phys.* **7**:200 (1939); W. Band, *J. Chem. Phys.* **7**:324, 927 (1939).
2. F. F. Abraham, *Homogeneous Nucleation Theory* (Academic Press, New York, 1974); A. C. Zettlemoyer, ed., *Nucleation* (Marcel Dekker, New York, 1969), A. C. Zettlemoyer, ed., *Nucleation Phenomena* (Elsevier, New York, 1977).
3. T. L. Hill, *Statistical Mechanics* (McGraw-Hill, New York, 1956), Chap. 5.
4. D. E. Strogyn and S. H. Hirschfelder, *J. Chem. Phys.* **31**:1531 (1959).
5. W. H. Zurek and W. C. Schieve, *J. Chem. Phys.* **73**:4061, 4663 (1980).
6. S. M. T. de la Selva, R. Dickman, W. C. Schieve, and C. Canestaro, *J. Chem. Phys.* **78**:6885 (1983).
7. W. J. Dunning, in *Nucleation*, A. C. Zettlemoyer, ed. (Marcel Dekker, New York, 1969), p. 1.
8. H. Reiss, in *Nucleation Phenomena*, A. C. Zettlemoyer, ed. (Elsevier, New York, 1977), p. 1.
9. K. A. Nishioka, *Phys. Rev. A* **16**:2143 (1977).
10. J. K. Lee, F. F. Abraham, and G. M. Pound, *Surf. Sci.* **34**:745 (1973).
11. F. F. Abraham and J. V. Dave, *J. Chem. Phys.* **55**:1587, 4817 (1971).
12. J. J. McGinty, *J. Chem. Phys.* **55**:580 (1971); M. R. Hoare, P. Pal, and P. P. Wegener, *J. Collect. Int. Sci.* **75**:126 (1980); N. G. Garcia and J. M. Torroja, *Phys. Rev. Lett.* **47**:186 (1981).

13. J. Lothe and G. M. Pound, *J. Chem. Phys.* **36**:2080 (1962).
14. O. Penrose and J. L. Lebowitz, in *Fluctuation Phenomena*, E. W. Montroll and J. L. Lebowitz, eds. (North-Holland, Amsterdam, 1979), p. 293.
15. C. Domb, *J. Phys. A Math. Gen.* **9**:283 (1976); C. Domb, *Ann. Israel Phys. Soc.* **2**:61 (1978).
16. M. E. Fisher, *Physics* **3**:255 (1967).
17. K. Binder, in *Phase Transitions and Critical Phenomena*, Vol. 5B, C. Domb and M. S. Green, eds. (Academic Press, New York, 1976), p. 1.
18. K. Binder and M. H. Kalos, *J. Stat. Phys.* **22**:363 (1980).
19. R. Dickman and W. C. Schieve, *Physica* **112A**:51 (1982).
20. M. F. Sykes and M. Glen, *J. Phys. A Math. Gen.* **9**:87 (1976).
21. R. Ziff, short talk at 47th Statistical Mechanics Meeting, Rutgers University, May, 1982.
22. R. C. Tolman, *J. Chem. Phys.* **17**:333 (1949).
23. R. Peierls, *Proc. Cambridge Philos. Soc.* **32**:477 (1936).
24. R. C. Heitmann and C. Radin, *J. Stat. Phys.* **22**:281 (1980).